ANL/NE-16/31

Bentonite-Clay Waste Form for the Immobilization of Cesium and Strontium from Fuel Processing Waste Streams

Nuclear Engineering Division

About Argonne National Laboratory
Argonne is a U.S. Department of Energy laboratory managed by UChicago Argonne, LLC under contract DE-AC02-06CH11357. The Laboratory's main facility is outside Chicago, at 9700 South Cass Avenue, Argonne, Illinois 60439. For information about Argonne and its pioneering science and technology programs, see www.anl.gov.

DOCUMENT AVAILABILITY

Online Access: U.S. Department of Energy (DOE) reports produced after 1991 and a growing number of pre-1991 documents are available free via DOE's SciTech Connect (http://www.osti.gov/scitech/)

Reports not in digital format may be purchased by the public from the National Technical Information Service (NTIS):

U.S. Department of Commerce
National Technical Information Service
5301 Shawnee Rd
Alexandria, VA 22312
www.ntis.gov
Phone: (800) 553-NTIS (6847) or (703)
605-6000 Fax: (703) 605-6900
Email: **orders@ntis.gov**

Reports not in digital format are available to DOE and DOE contractors from the Office of Scientific and Technical Information (OSTI):

U.S. Department of Energy
Office of Scientific and Technical Information
P.O. Box 62
Oak Ridge, TN 37831-0062
www.osti.gov
Phone: (865) 576-8401
Fax: (865) 576-5728
Email: **reports@osti.gov**

Disclaimer
This report was prepared as an account of work sponsored by an agency of the United States Government. Neither the United States Government nor any agency thereof, nor UChicago Argonne, LLC, nor any of their employees or officers, makes any warranty, express or implied, or assumes any legal liability or responsibility for the accuracy, completeness, or usefulness of any information, apparatus, product, or process disclosed, or represents that its use would not infringe privately owned rights. Reference herein to any specific commercial product, process, or service by trade name, trademark, manufacturer, or otherwise, does not necessarily constitute or imply its endorsement, recommendation, or favoring by the United States Government or any agency thereof. The views and opinions of document authors expressed herein do not necessarily state or reflect those of the United States Government or any agency thereof, Argonne National Laboratory, or UChicago Argonne, LLC.

ANL/NE-16/31

Bentonite-Clay Waste Form for the Immobilization of Cesium and Strontium from Fuel Processing Waste Streams

---

by
Michael D. Kaminski and Carol J. Mertz
Nuclear Engineering Division, Argonne National Laboratory

October 2016

CONTENTS

FIGURES

FIGURES (CONT.)

TABLES

BENTONITE-CLAY WASTE FORM FOR THE IMMOBILIZATION OF CESIUM AND STRONTIUM FROM FUEL PROCESSING WASTE STREAMS

M.D. Kaminski and C. J. Mertz
Nuclear Engineering Division
Argonne National Laboratory

ABSTRACT

The physical properties of a surrogate waste form containing cesium, strontium, rubidium, and barium sintered into bentonite clay were evaluated for several simulant feed streams: chlorinated cobalt dicarbollide/polyethylene glycol (CCD-PEG) strip solution, nitrate salt, and chloride salt feeds. We sintered bentonite clay samples with a loading of 30 mass% of cesium, strontium, rubidium, and barium to a density of approximately 3 g/cm^3. Sintering temperatures of up to 1000°C did not result in volatility of cesium. Instead, there was an increase in crystallinity of the waste form upon sintering to 1000ºC for chloride- and nitrate-salt loaded clays. The nitrate salt feed produced various cesium pollucite phases, while the chloride salt feed did not produce these familiar phases. In fact, many of the x-ray diffraction peaks could not be matched to known phases. Assemblages of silicates were formed that incorporated the Sr, Rb, and Ba ions. Gas evolution during sintering to 1000°C was significant (35% weight loss for the CCD-PEG waste-loaded clay), with significant water being evolved at approximately 600°C.

1 INTRODUCTION

The Global Nuclear Energy Partnership (GNEP) describes a closed fuel cycle strategy that will require the separation and emplacement of a variety of reprocessing waste streams. The solvent extraction process being developed to produce these separated waste streams, the Uranium Extraction process or UREX, may produce a single stream containing cesium, strontium, rubidium, and barium together in either an acidic nitrate media or an organic carbonate media with a complexing agent (diethylene triamine pentaacetic acid or DTPA). The cesium and strontium waste solution from a pyrochemical processing flowsheet will be composed of chloride salts. These streams must be stabilized and the radionuclides stored until they can be disposed. In earlier publications, we described the thermal properties of potential storage media [Kaminski 2005a] and the estimated storage form volumes and potential storage scenarios [Kaminski 2005b]. However, those studies were performed based on theoretical properties since the fabrication of such engineered products is largely novel.

One can envision many candidate matrices for potentially stabilizing the radionuclides. Within the GNEP program, the decision was made to study alumino-silicate host materials initially and processes for preparing these waste form matrices. There are no published studies on the properties of sintered alumino-silicates containing a mixture of cesium in combination with alkali and alkaline earth metals. However, there is an abundance of information on the formation of pollucite from cesium solutions and alumino-silicates. To produce pollucite, Strachan and Shulz [Strachan 1976] described the formation of pollucite directly from sintering a cesium chloride solution in bentonite clay. They found that 750°C for 2 h was required to convert CsCl mixed with bentonite clay into pollucite, and the use of caustic cesium chloride and precalcining the bentonite lowered the temperature for complete reaction to <650°C. The maximum loading of Cs to form pollucite was 42.6%. One more recent study [MacLaren 1999] described a multi-step process with cesium hydroxide, water, aluminum, powder, and SiO_2 as starting materials to prepare a sol which was hydrothermally processed at 220°C for 2-24 h to produce a dry powder. MacLaren et al. achieved 95% theoretical density after sintering at 1500°C for 10 h. Yanagisawa et al. [Yanagisawa 1987] created pollucite structures for cesium by hydrothermal alteration of alumino-silicate, quartz, and $Al(OH)_3$. They found that pollucite could be formed at 200°C under alkaline conditions. Their results also suggest that the cesium anion might play a significant role in the leaching characteristics of cesium pollucite.

We describe here alumino-silicates prepared by dry-sintering bentonite clay containing cesium, strontium, rubidium, and barium salts. We investigated the physical properties of various pressed and sintered samples, some basic thermal properties, and the gas evolved during sintering. We noted the release of water with a peak in its evolution at approximately 600°C. This was accompanied by NO_x species. The crystallinity of the waste form increased with increasing temperature up to 1000°C as evidenced by x-ray diffraction. The final waste product was hard and brittle with a true density of 3 g/cm^3, 44% porosity, and loading of 29 mass% of cesium, strontium, rubidium, and barium.

2 METHODS

Deionized water was obtained from an in-house supply. The strontium nitrate and chloride salts were reagent grade. The bentonite clay was a sodium bentonite (Volclay HPM-20, 425 mesh, American Colloid Company, Belle Fourche, SD) that was air purified and classified at the plant. It contained 12% moisture and was used as received. The technical data sheet provided the elemental composition of the material, which was corroborated by x-ray fluorescence (XRF) data provided by the University of Nevada Las Vegas (personal communication with Dr. Gary Cerefice, Harry Reid Center, UNLV). The moisture free composition reported by American Colloid was SiO_2=69.56%, Al_2O_3=20.69%, MgO=2.70%, Fe_2O_3=4.85%, CaO=1.30%, Na_2O=2.43%, K_2O=0.30%. The loss-on-ignition was 4.80%. The specific gravity was 2.6, and the pH of a 2% solid suspension was 8.5-10.5.

2.1 CESIUM AND STRONTIUM WASTE FEED COMPOSITIONS

Bentonite clay samples were prepared based upon the work of Strachan and Shulz [Strachan 1976]. A maximum loading of 42.6% cesium was obtained upon loading a 3$\underline{M}$ CsCl waste stream to bentonite clay and by sintering to form pollucite [Strachan 1976]. In addition to Cs, the waste feed in this study included Rb, Ba, and Sr. Thus, a stock solution was prepared to compensate for the other cations that would occupy sorption sites within the clay. The Sr concentration was obtained from the ratio in the chlorinated cobalt dicarbollide/polyethylene glycol (CCD-PEG) strip solution (approximately 0.2 g/L Cs and 0.1 g/L Sr), and the Ba and Rb concentrations were obtained from mass ratios for Cs/Rb = 3340/537 and Sr/Ba = 1180/3100 from ORIGEN calculations for 10-y old fuel burned to 50 GWd/MT (4.25% enriched).

A chloride-feed stock solution was prepared with 0.565$\underline{M}$ Cs^+, 0.427$\underline{M}$ Sr^{2+}, 0.141$\underline{M}$ Rb^+, and 0.719$\underline{M}$ Ba^{2+} (as the chloride salts).

The nitrate-feed stock solution for maximum waste loading of the clay was prepared using nitrate salts at one-fifth the chloride waste stream concentrations of the alkali and alkaline earth elements due to the limited solubility of the nitrate salts of Cs and Ba.

An additional aqueous feed to the waste solidification process was prepared based upon the strip solution concentrations from the CCD-PEG process (CCD-PEG simulated strip solution) using the same elemental ratios for the alkali and alkaline earth waste elements as the maximum waste-loaded clay. From the UREX+ process flowsheet, the cesium and strontium waste stream has concentrations of approximately 100 g/L guanidine carbonate and 20 g/L diethylene triamine pentaacetic acid (DTPA), in addition to some nitric acid from the process scrub solution (3$\underline{M}$ HNO_3). The CCD-PEG stock solution was prepared with the following composition: 0.293 g/L $CsNO_3$, 0.242 g/L $Sr(NO_3)_2$, 0.0555 g/L $RbNO_3$ and 0.500 g/L $Ba(NO_3)_2$, 100 g/L guanidine carbonate, and 20 g/L DTPA.

2.2 SAMPLE PREPARATION FOR BENTONITE CLAY LOADED WITH CCD-PEG SIMULATED STRIP SOLUTION

To a 5-g sample of bentonite clay was added approximately 10 mL of the CCD-PEG simulated strip solution (composition defined in previous section). This mixture was homogenized with a glass stir rod and dried at 50°C overnight. The dried clay sample was mixed by mortar and pestle, and a portion of the sample was submitted for off-gas and thermal gravimetric (TGA) analyses.

2.3 SAMPLE PREPARATION FOR BENTONITE CLAY LOADED WITH THE CHLORIDE AND NITRATE SALT FEED SOLUTION

The chloride feed solution (27.9 mL, 0.565$\underline{M}$ Cs^+, 0.427$\underline{M}$ Sr^{2+}, 0.141$\underline{M}$ Rb^+, and 0.719$\underline{M}$ Ba^{2+}) was added to 15 g of clay, mixed to homogenize, and dried overnight at 60°C. In addition, this solution was diluted by 2 and 4 and added in the same proportion to produce samples at progressively lower loadings.

For the nitrate feed solution in the clay, the nitrate feed solution (27.9 mL, 1/5 the chloride cation concentration) was added to 15 g of clay, the mixture was homogenized, and dried overnight at 60°C, and this process was repeated for a total of 5 times. The dried waste-loaded clay samples were mixed by mortar and pestle, and samples were prepared for analyses based upon the respective techniques.

2.4 SAMPLE PRESSING AND SINTERING

Using the bentonite clay samples prepared with the chloride-based feed solution, we sintered a variety of right cylindrical pucks. Pucks were prepared after drying the salt-loaded clay samples at 60°C and powdering them by mortar and pestle. This powder was added to the die (pre-coated with 3% stearic acid in ethanol), pressed by hand, and then pressed in a mechanical press (Carver 24,000 lb). The powder was pressed (either 0.5 inch, 0.634 inch, 0.75 inch, or 1-1/8 inch diameter dies) at 5000, 7900, 10,000, or 15,000 psi. Then, samples were heated from room temperature at 5°C/min in a Lindberg Blue Furnace or Fisher Scientific Isotemp® Programmable Furnace calibrated against pyrometric cones (Orton Ceramics, Westerville, Ohio). Samples were kept at peak temperature (600-1000°C) for 12 h and slowly cooled (5°C/min) to room temperature.

2.5 BULK DENSITY

The bulk density of pressed and sintered samples was calculated by measuring the geometric dimensions of the cylindrical sample using digital calipers (Mitutoyo Digimatic Caliper) and weighing the sample (Mettler balances).

2.6 POROSITY

The open porosity density (true density) of pressed and sintered samples was measured using a Micropycnometer (Quantachrome, MPY-5) run with pure helium gas. A monolithic or crushed sample was placed in the sample cell and weighed. The sample was placed in the cell holder and sealed. The instrument compared the pressure difference between a known quantity of helium in a reference cell volume V_R and that of the helium when it was released into the sample cell V_c to determine the volume of sample V_p. Two grab samples were analyzed, and the average value and range was reported. The instrument was calibrated against standard stainless steel spheres. The porosity was calculated as:

$$V_p = V_c - V_R \left(\frac{P_1}{P_2} - 1 \right) \tag{1}$$

where P_1 was the pressure in the reference cell, and P_2 was the pressure in the sample cell. The average of three measurements is reported. To check the accuracy of this unit against monolithic samples and confirm that the true density was being measured, some samples were crushed, and their density compared to their monolithic measurements. They were in agreement in all cases. The porosity was calculated from the ratio of the bulk and true density.

2.7 ELECTRON MICROSCOPY

Clay samples were ground to a coarse powder, sprinkled onto a carbon sticky tape, and mounted on an aluminum stub for analysis. Samples were analyzed without further treatment. We used a Jeol JSM-6400 or Hitachi S-4700 scanning electron microscope at an accelerating voltage of 3-20 kV coupled to an energy dispersive x-ray analyzer.

2.8 ELEMENTAL ANALYSIS

Neutron activation analysis was performed on five bentonite clay samples. Samples were ground to a powder by mortar and pestle, sealed in polyethylene capsules, and irradiated in a TRIGA reactor (University of Texas, Austin, TX). Four of the samples included cesium, barium, rubidium, and strontium nitrate salts loaded into the clay. They were processed as follows: (1) unsintered, (2) sintered at 600°C, (3) sintered at 800ºC, and (4) sintered at 1000°C. The fifth sample was a control consisting of the bentonite clay. Barium and strontium were analyzed on triplicate samples in the thermal neutron pneumatic transfer system (tPNT) mode at 165.8 keV for Ba-139 and at 388 keV for Sr-87m. Cesium and rubidium were analyzed on duplicate samples in the rotary specimen rack (RSR) mode at 604.7 and 795.8 keV for Cs-134 and at 1077 keV for Rb-86.

2.9 THERMAL CONDUCTIVITY

Thermal conductivity testing was performed at 300-1000°C. Thermal diffusivity (α) was measured by laser flash technique. Specific heat (C_p) was measured with a differential scanning calorimeter. The thermal conductivity was calculated from $k=\alpha C_p$. In the flash method, the front face of the disc-shaped sample was exposed to a short laser pulse, and the resulting rear face temperature rise was recorded and analyzed. Specific heat was measured with sapphire as the standard reference material. The standard and sample were subjected to the same heat flux as a blank, and the differential powers required to heat the sample and standard at the same rate were determined by the digital acquisition system. From the masses of the sapphire standard and sample, the differential power, and the known specific heat of sapphire, the specific heat of the sample was computed.

2.10 X-RAY DIFFRACTION

Samples were analyzed by x-ray diffraction using a Rigaku D/max Rotating Anode Diffractometer equipped with a vertical goniometer employing copper Kα radiation. The software program used to analyze the diffraction pattern was Jade 5.0 (Materials Data, Inc.). It used standard search/match parameters to compare the unknown diffraction pattern against powder diffraction patterns supplied by the International Centre for Diffraction Data. Diffractions patterns were obtained under the following conditions: operating parameters: 40 kV, 175 mA; scan speed: 2.4 degrees/min; scan angle: 10-80 degrees.

2.11 THERMAL GRAVIMETRIC AND DIFFERENTIAL THERMAL ANALYSES

The 10.82 mg of the sample was taken in a 70 µl alumina pan and heated from 25 to 800°C in a thermogravimetric analyzer (Mettler Toledo TGA/SDTA 851E) at a rate of 5°C/min in nitrogen atmosphere or air with a flow rate of 60-90 mL/min.

2.12 OFF-GAS ANALYSIS

The temperature-programmed gas evolution studies were conducted by measuring the product yield as a function of temperature using a commercial characterization system (Zeton Altamira, Model AMI-100). A powder sample of 100 mg was heated from room temperature to 1000°C at a rate of 2°C/min in a gas mixture of 4% O_2 in He at a flow rate of 50 mL/min. The temperature was monitored with an Omega Type K thermocouple located at the exit of the sample bed. The product gas concentration was analyzed for CO, CO_2, H_2O, NH_3, NO, NO_2, N_2O, HCN, Cs, and CsOH using a Dycor Dymaxion quadrupole mass spectrometer. The analyses were limited to species with formula weights less than 200.

3 RESULTS

The bentonite clay was off-white in color and sintered to a friable rust-orange mass (Figure 1, left). When loaded with the surrogate radionuclides (29 mass% of Cs, Sr, Rb, and Ba), it sintered to a yellow-white mass that was less friable (Figure 1, right). The radial compaction of the samples was 2-4% at 1000°C, but the radius increased by 2% when sintered at 800°C. When we decreased the loading of surrogate radionuclides into the bentonite, the compaction increased slightly, being 6% at 8.4 wt% loading. The overall density of the alumino-silicate was affected by the loading of surrogate radionuclides (Table 1). Higher loading led to higher porosity, higher true density, but lower bulk density.

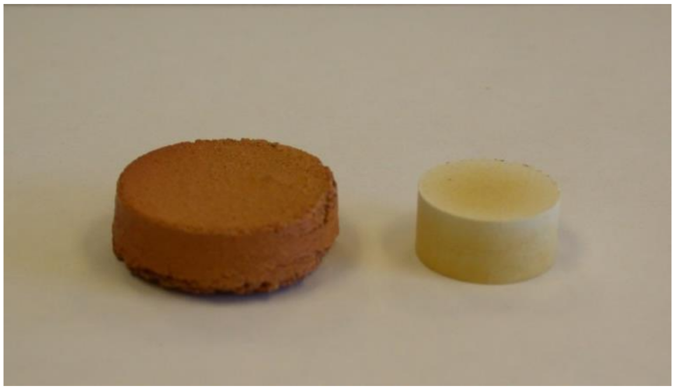

FIGURE 1 Sintered bentonite clay (left) and sintered bentonite containing Cs, Sr, Rb, and Ba chloride waste feed (right, 29% waste loading).

TABLE 1 Porosity of chloride-loaded waste of sintered bentonite monoliths containing radionuclide surrogates (chloride salts of Cs, Sr, Rb, and Ba) at different waste loadings.

Sample	Waste Loading (%)	Bulk Density (g/cm^3)	True Density (g/cm^3)	Porosity
Chloride salt loaded	29	1.61	3.05	47%
Chloride salt loaded	16	1.82	2.83	36%
Chloride salt loaded	8	2.07	2.63	21%

3.1 CONSOLIDATION PRESSURE

The pressure that was used to consolidate the cold material had little effect on the true density, while the bulk density increased slightly when pressed to >5000 psi (Figure 2). The resulting porosity was slightly affected. We observed a porosity of 44% at 5000 psi compared to 36% at 15,000 psi. When the sintering temperature was increased from 600 to 1000°C, we did not observe a significant difference in the bulk or true density or the resulting porosity for samples consolidated to 5000 psi. (Data are shown in Appendix, Table A1).

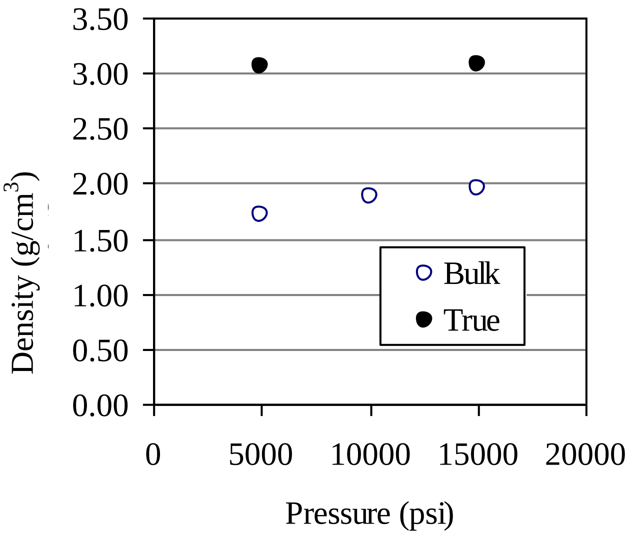

FIGURE 2 Storage form surrogate density as a function of consolidation pressure of the green compact.

3.2 THERMAL PROPERTIES

We measured the thermal properties of the bentonite clay loaded with 29 mass% of Cs, Sr, Rb, and Ba from the chloride-based salt solution. The thermal diffusivity of this material was not sensitive to temperature up to 1000°C (Figure 3). However, the specific heat of the material increased by 42% over the same range. The thermal conductivity (Figure 4) increased from 1.5 W/m/K to 1.95 W/m/K as the temperature was increased to 1000°C. This result was rather surprising given the high porosity of the sample (~45%). According to the computational model [Kaminski 2005a], at this porosity, the thermal conductivity of air prevents a porous solid from achieving a thermal conductivity greater than 0.5 W/m/K, even if the theoretically dense material has a k = 20 W/m/K. This computational prediction was checked against a model developed by Singh et al. [Singh 1995], which describes heat conduction in a two-phase system by using an analogy with electrical resistance. The derived equation predicts an effective thermal conductivity k_e, which is a function of the thermal conductivity of the theoretically dense solid and the fluid, and a semi-empirical equation called the “porosity correction factor,” which was fit to a number of data sets for various solids and fluids. Their model was in excellent agreement

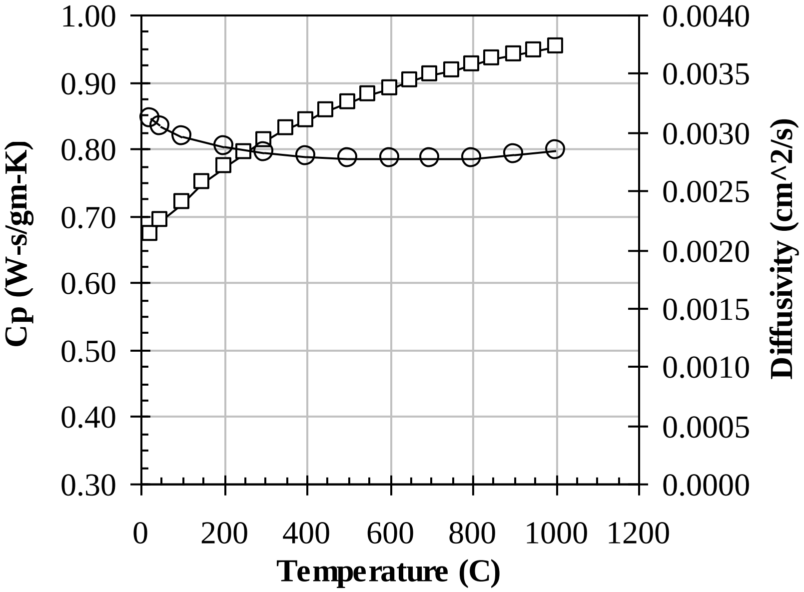

FIGURE 3 Specific heat (squares) and thermal diffusivity (circles) of sintered bentonite (1000°C) containing 29 mass% of Cs, Sr, Rb, and Ba as chloride salts.

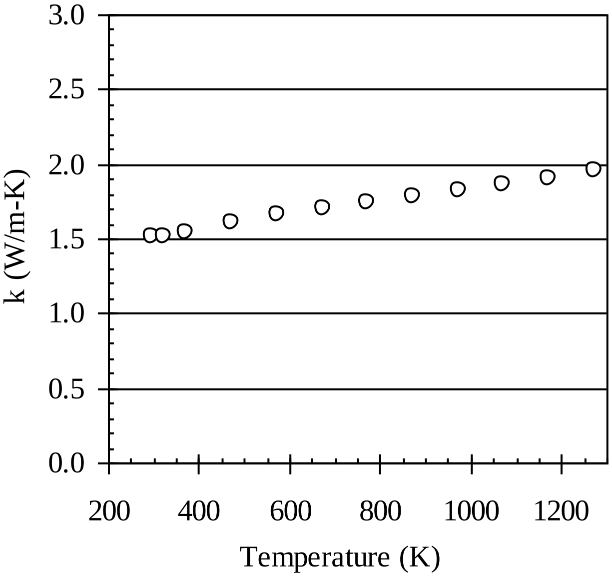

FIGURE 4 Thermal conductivity of sintered bentonite (1000°C) containing 29 mass% of Cs, Sr, Rb, and Ba as chloride salts.

with reported experimental values. Using Singh's approach, we calculated that the effective thermal conductivity of the alumino-silicate differed from that of the Kaminski model [Kaminski 2005a] by only 0.03 W/m/K. Therefore, the source of discrepancy must be elsewhere.

From these data we determined the temperature dependence of the thermal conductivity for input into a computational model [Kaminski 2005a] for calculating the temperature profile for long cylinders of storage material. The thermal resistivity *R*, which is the reciprocal of k, of ceramic oxides typically follow a linear relationship with temperature due predominantly to phonon scattering. where R = 1/k =A+ BT, where A and B are constants. For the sintered bentonite (Figure 5), the correlation (B=-0.000153, A=0.699, R^2=0.98) was very good.

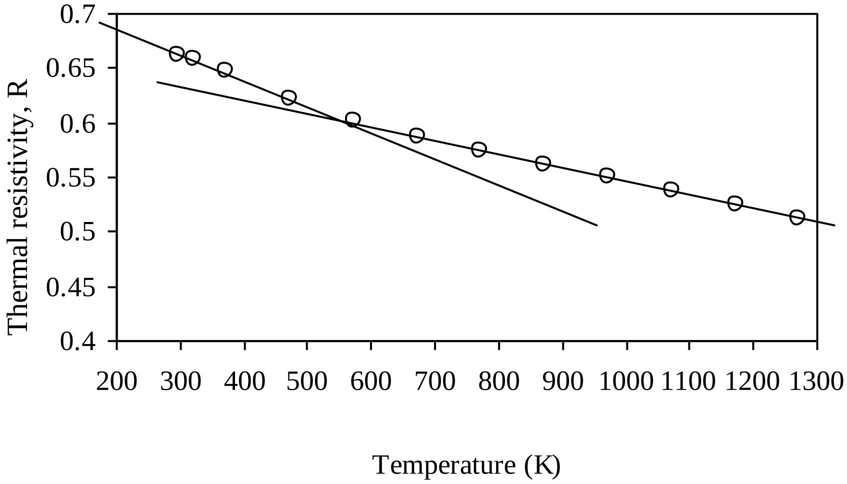

FIGURE 5 Thermal resistivity of sintered bentonite (1000°C) containing 29 mass% of Cs, Sr, Rb, and Ba as chloride salts..

3.3 SINTERING TEMPERATURE AND WASTE LOADING

Neutron activation analysis (NAA) was performed on bentonite clay samples loaded with Cs, Sr, Ba, and Rb nitrates as a function of sintering temperature. The NAA indicated no volatility of cesium based upon the elemental concentrations in unsintered and heat-treated samples (shown in Table 2). The control sample (bentonite clay) showed no significant concentration of the waste components (Cs, Sr, Rb, and Ba). In addition, no significant change in the waste component concentrations (Cs, Rb, Sr, Ba) was found as a function of sintering temperature (600 to 1000ºC). The changes in concentration are within the measurement error. All waste component concentrations in the sintered samples increased by 25% when compared with the unsintered, waste-loaded clay sample. This increase can be accounted for in the water and nitrous oxides losses that occurred during sintering of the clay samples.

TABLE 2 Neutron activation analysis results for bentonite clay samples loaded with nitrate salt feed containing Cs, Sr, Rb, and Ba.

Sample Description	Waste Loading (%)	Rb (µg/g)		Cs (µg/g)		Ba (µg/g)		Sr (µg/g)	
		Conc.	Error	Conc.	Error	Conc.	Error	Conc.	Error
Bentonite clay	0			22	1.13			369	154
Unsintered	29.4	13018	282	70446	339	99132	1070	37265	598
600°C	29.4	16227	350	88739	427	116111	1249	44089	702
800°C	29.4	16408	352	89408	430	122435	1339	46089	766
1000°C	29.4	16327	356	87858	423	119380	1287	45693	729

Note: Conc. (concentration) and error are average values.

3.4 MINERAL COMPOSITION

We used x-ray diffraction to monitor the mineral composition and crystallinity of the clay material loaded with chloride and nitrate waste as a function of sintering temperature. The x-ray data for the chloride-loaded clay material showed a distinct transformation above 700°C, noted by the decrease in the amorphous scattering background at low 2θ (Figure 6). From the plots we could identify several peaks such as barium, strontium, and aluminum silicates, but few others could be identified with a high degree of confidence. Interestingly, no pollucite was formed. To investigate this further, we prepared samples with progressively lower concentrations of surrogate radionuclides to see if pollucite would form at lower waste loadings (Figure 7). There was an absence of the pollucite signature peaks even at 25% of theoretical waste loading of the clay.

A diffraction pattern for the bentonite clay starting material (Figure 8) identified montmorillonite as the major phase. In addition, quartz and potassium aluminum silicate phases were identified (Figure 9). A relatively large amorphous or nanocrystalline component was present in the clay, as indicated by the peak broadening.

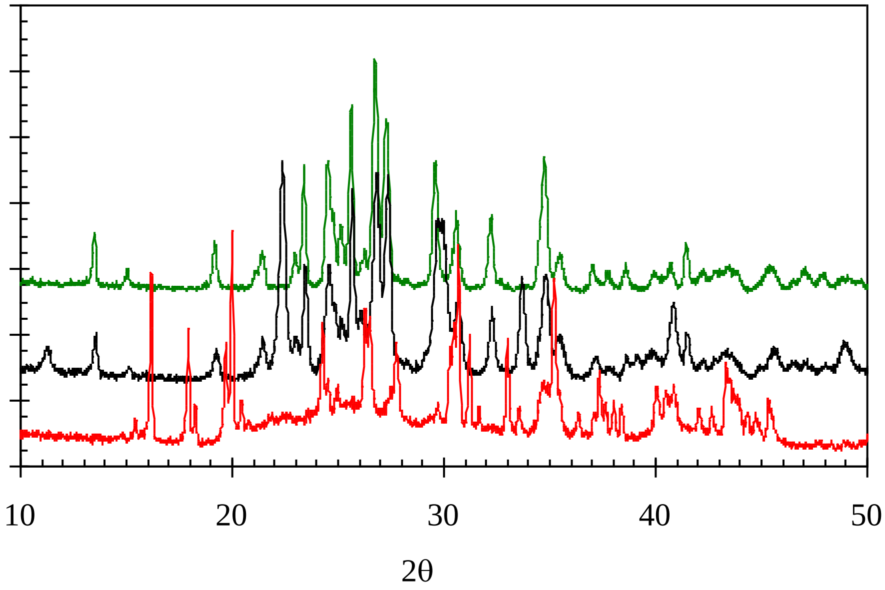

FIGURE 6 X-ray diffraction pattern of sintered bentonite containing 29 mass% of Cs, Sr, Rb, and Ba as chloride salts at 1000°C (top), 800°C (middle), and 600°C (bottom). The 700°C data (not included) are similar to the 600°C data.

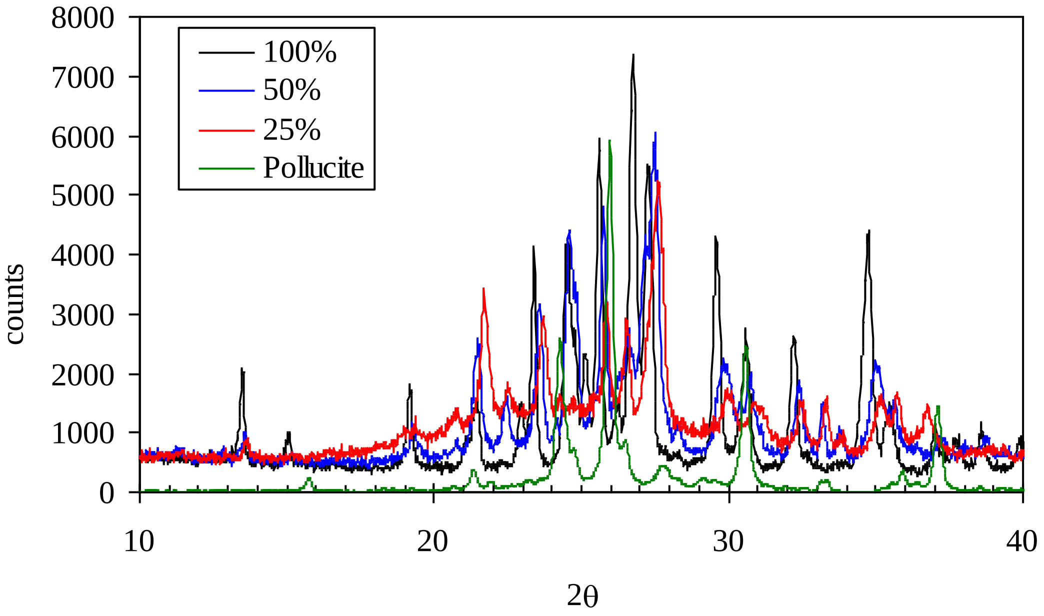

FIGURE 7 X-ray diffraction pattern of sintered bentonite (1000°C) containing Cs, Sr, Rb, and Ba as chloride salts. Loading of salt varied from 100% to 25% theoretical limit (29 mass% to 8 mass% Cs, Sr, Rb, and Ba). The pollucite diffraction pattern is shown.

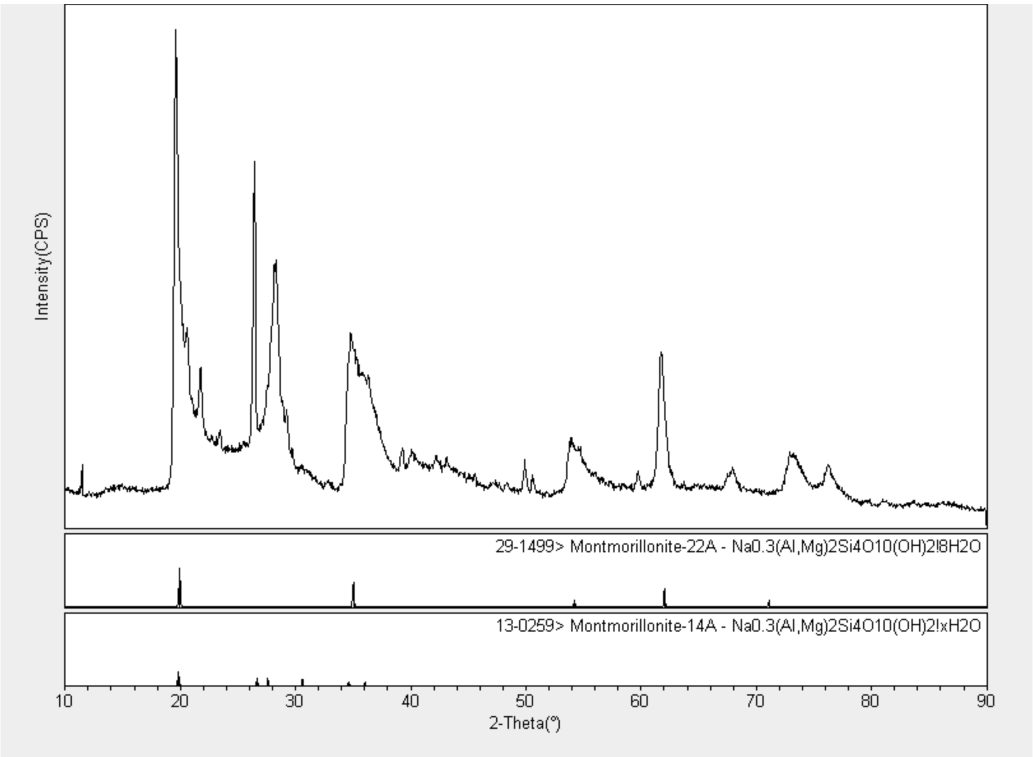

FIGURE 8 X-ray diffraction pattern of bentonite clay showing montmorillonite.

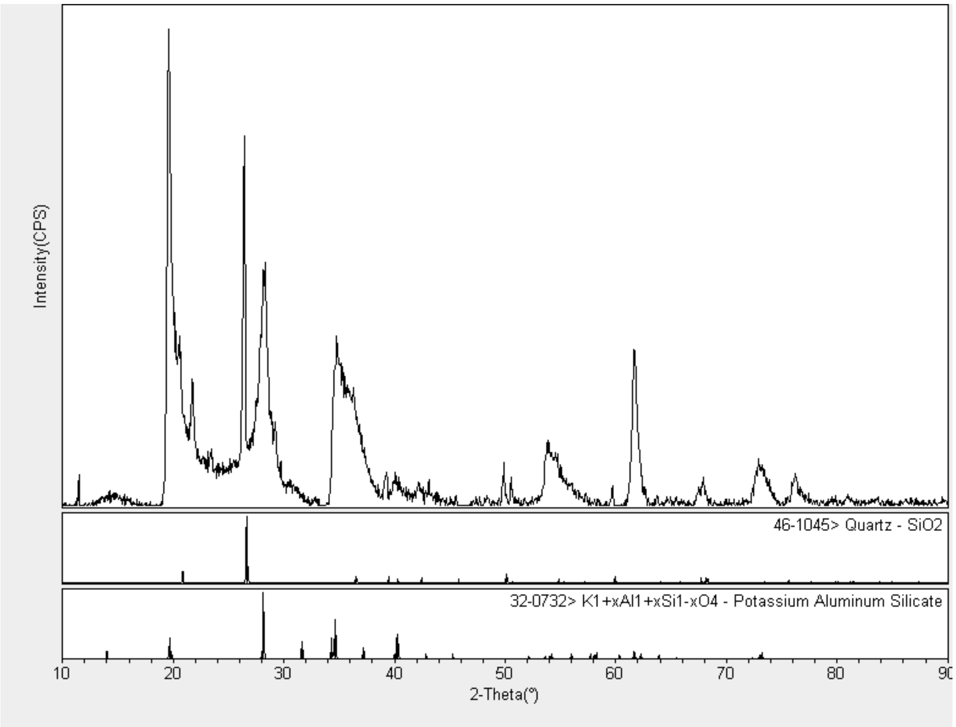

FIGURE 9 X-ray diffraction pattern identifying quartz and potassium aluminum silicate in the bentonite clay.

The mineral composition and crystallinity of nitrate-loaded (29 mass% Cs, Sr, Rb, and Ba) bentonite clay were also monitored by x-ray diffraction. Analysis of the nitrate-loaded, unsintered clay produced an x-ray diffraction pattern that matched magnesium/iron silicate, strontium nitrate, and barium nitrate phases (Figure 10). Upon heating to 600°C, celsian (barium aluminum silicate) formed (Figure 11). The clay underwent a transformation consistent with the heat treatment conformation of montmorillonites resulting from the loss of lattice water at ~600°C [Carrado 1991]. At 800°C, cesium-pollucite and hydroxyapophyllite were identified (Figure 12). An additional Fe-containing pollucite phase, rubidium iron silicate, and orthoclase appeared at 1000°C and, possibly, small amounts of barium/strontium aluminum silicates (Figure 13). An overlay of the unsintered and sintered (600-1000°C) nitrate-loaded bentonite clay samples (Figure 14) shows the increase in crystallinity upon sintering to 1000°C.

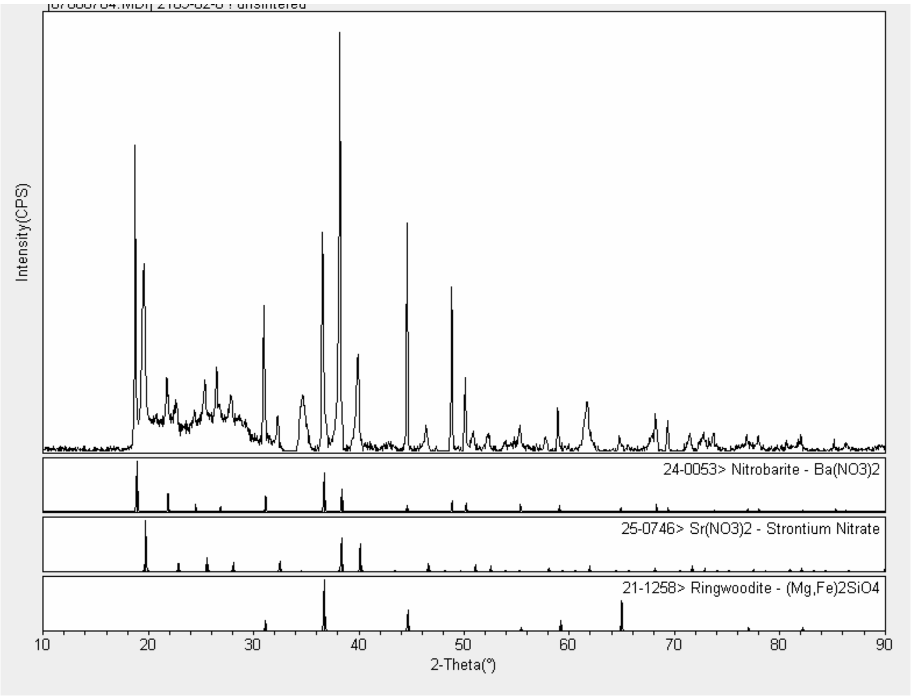

FIGURE 10 X-ray diffraction pattern for bentonite clay loaded with cesium, strontium, rubidium, and barium (29 mass% as nitrate salts). The sample was dried at 90°C, but not sintered.

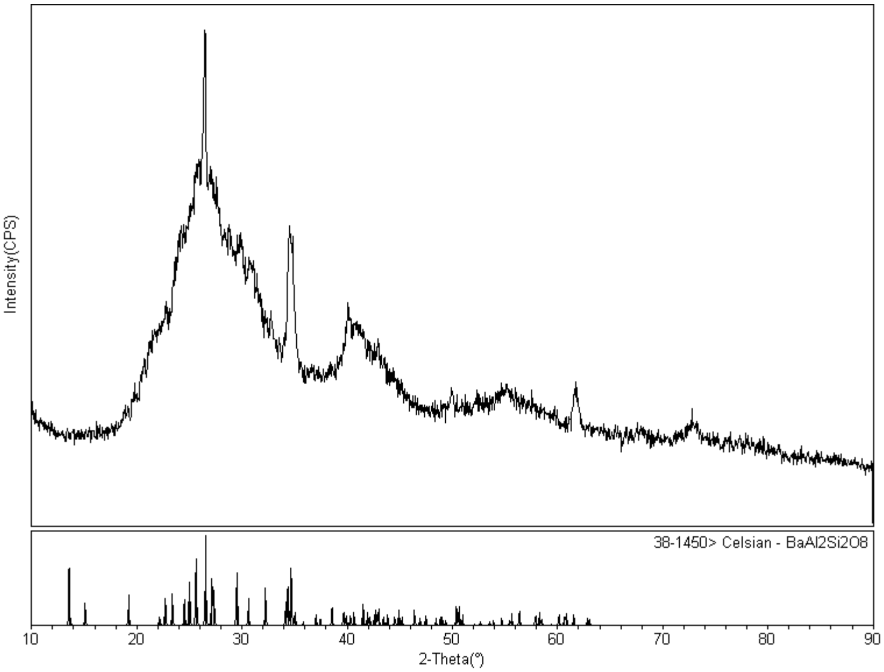

FIGURE 11 X-ray diffraction pattern for bentonite clay loaded with cesium, strontium, rubidium, and barium (29 mass% as nitrate salts). The sample was sintered at 600°C.

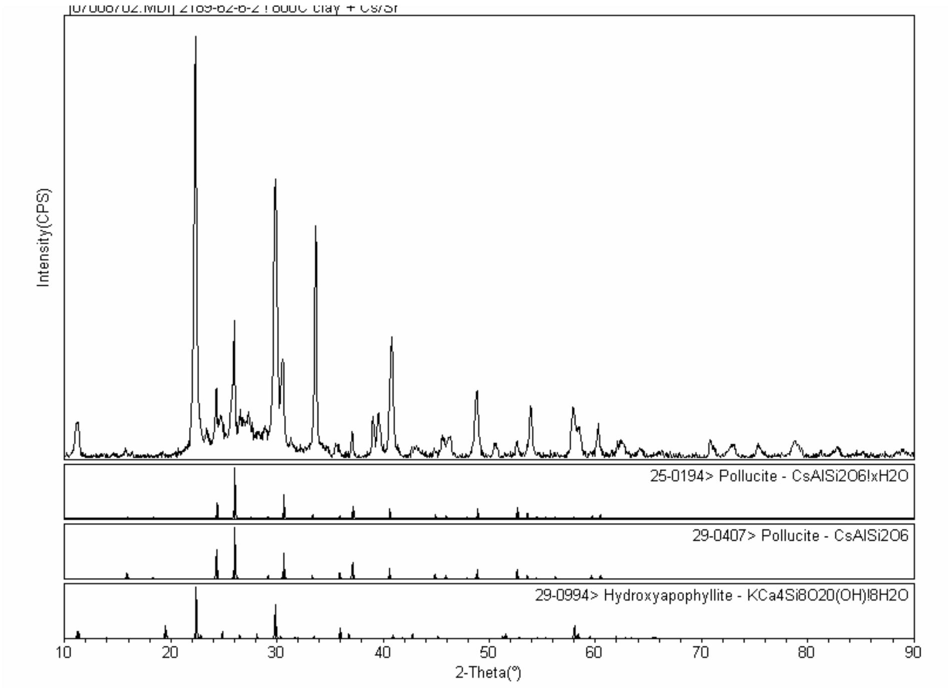

FIGURE 12 X-ray diffraction pattern for bentonite clay loaded with cesium, strontium, rubidium, and barium (29 mass% as nitrate salts). The sample was sintered at 800°C.

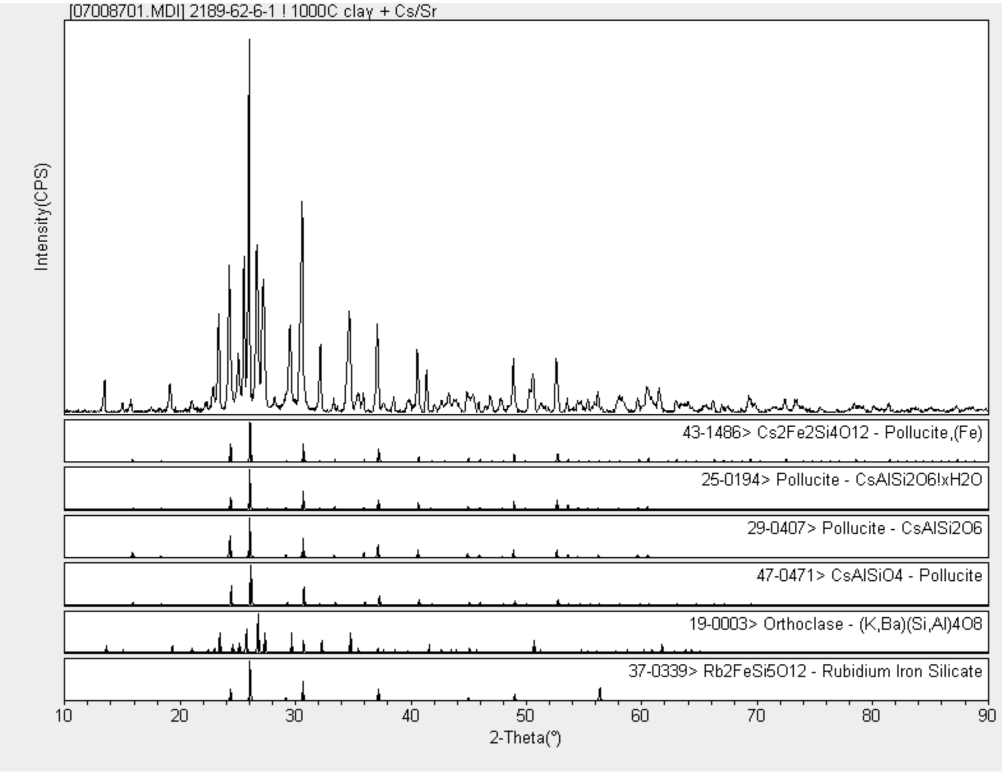

FIGURE 13 **X-ray diffraction pattern for bentonite clay loaded with cesium, strontium, rubidium, and barium (29 mass% as nitrate salts). The sample was sintered at 1000°C.**

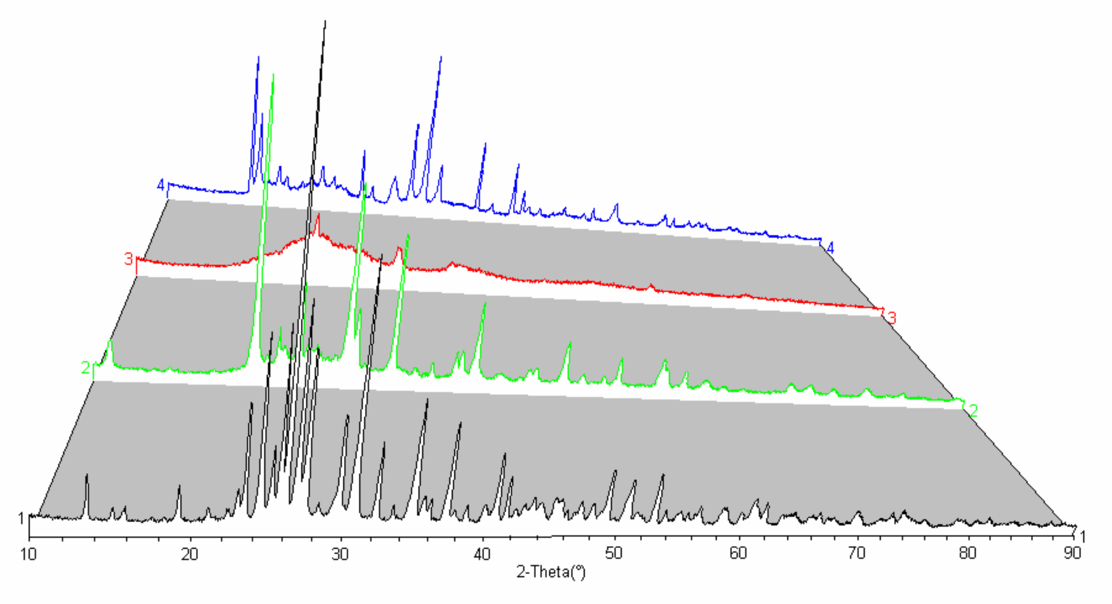

FIGURE 14 **X-ray diffraction patterns for bentonite clay loaded with cesium, strontium, rubidium, and barium (29 mass% as nitrate salts) as a function of sintering temperature: (1) 1000°C, (2) 800°C, (3) 600°C, and (4) unsintered.**

Comparison of the chloride- versus the nitrate-loaded bentonite clay sintered at 1000°C shows that the phases are different (Figure 15). The chloride-loaded clay consisted primarily of barium, strontium, and aluminum silicates while the nitrate-loaded clay was dominated by Cs-pollucite phases (Figure 15). An increase in crystallinity above 700ºC was observed with the chloride- and nitrate-loaded clays.

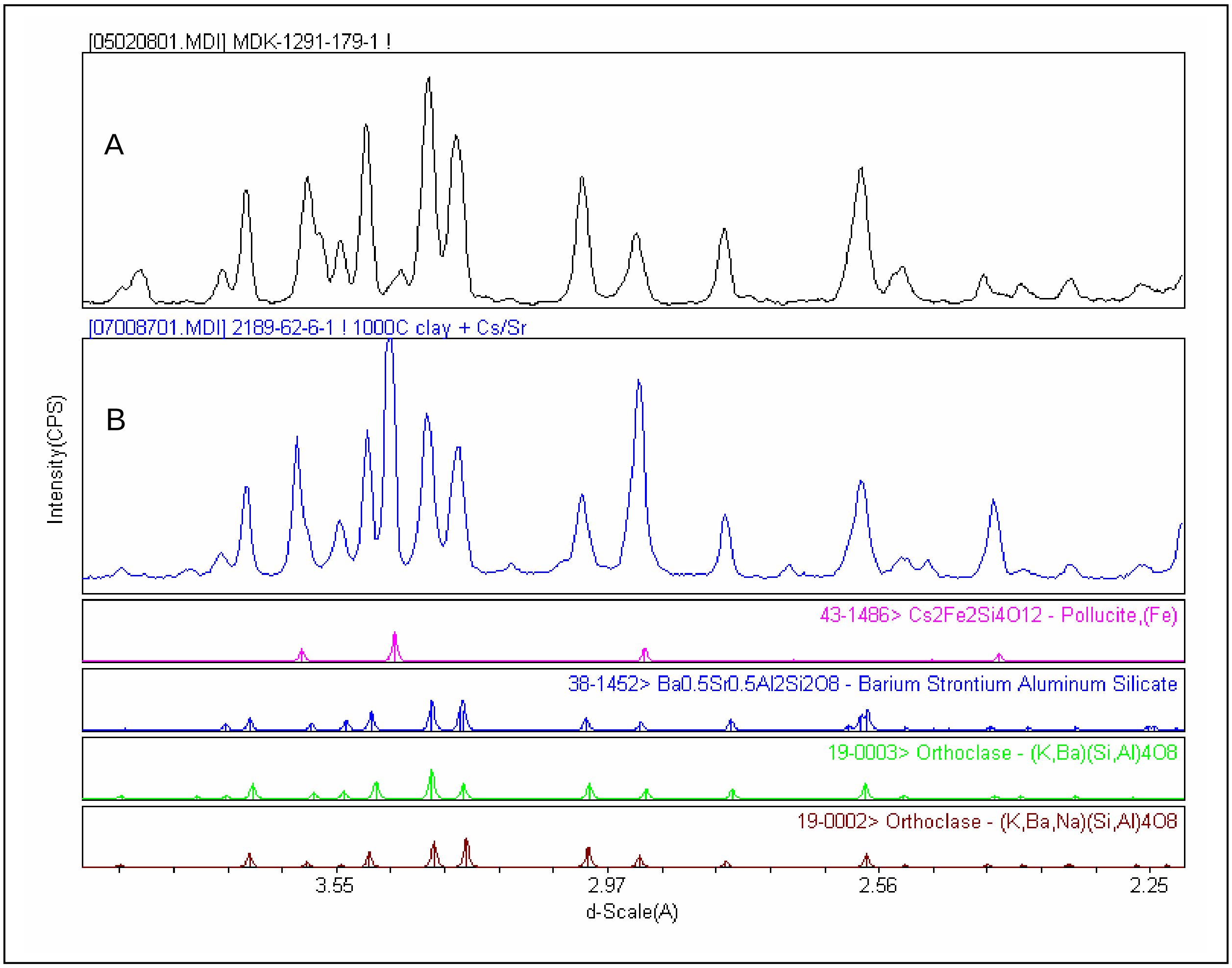

FIGURE 15 X-ray diffraction patterns of bentonite clay loaded with (A) chloride salts or (B) nitrate salts of cesium, strontium, rubidium and barium. Samples were waste loaded to 29% and sintered at 1000°C.

3.5 OFF-GAS ANALYSIS

We compared the composition of the gas evolved during sintering of bentonite clay samples loaded with Cs, Sr, Ba, and Rb from the CCD-PEG surrogate and the nitrate salt solution with that evolved from unloaded bentonite clay (Table 3). Cesium was not detected in the off-gas analyses for the waste-loaded clay samples for temperatures up to 900°C in 4% O_2/He (Figure 16). A major off-gas species for all the clay samples was water (Figure 17). All of the clay samples showed water losses at less than 100°C, indicating weakly-bound surface water. Additional water loss was detected at ~600°C for the clay and waste-loaded clay samples corresponding to dehydroxylation of the clay. Accompanied with the water loss ~600°C from the waste-loaded clay samples were other species. The nitric oxide species, NO (Figure 18), was a major off-gas component at 590°C from the nitrate-waste loaded clay, while CO_2 or N_2O species were a major component at 600°C for the CCD-PEG waste-loaded clay. Minor loss of interlayer water at 200 and 280°C from the CCD-PEG waste-loaded clay sample was associated with CO_2 or N_2O species (Figure 19) being lost over the same temperature range. Other nitrogen and carbon species were detected at much lower levels and were lost at temperatures corresponding to the major off-gas species (Table 3). These thermal transitions have previously been observed in clays containing organic compounds [Carrado 1991].

TABLE 3 Temperatures of peak maxima for off-gas species in waste-loaded bentonite clay samples. Comparison of off-gas species for bentonite clay and clay loaded with CCD-PEG simulated strip or nitrate salt feeds.

	Waste Loading		
Off-gas Species	None	CCD-PEG Feed	NO_3^- Feed
Cs	ND	ND	ND
CsOH	N/A	N/A	ND
H_2O	≤100, 675 (#)	≤100, 200, 280, 610 (#)	≤100, 590 (#)
N_2O, CO_2	630	200, 300, 460, 600 (#)	370, 550, >900
NO	ND	200, 300, 600	590 (#)
NO_2	ND	ND	580
CO, N_2	ND	200, 470, 600	350, 650

ND = none detected
N/A = not analyzed
(#) = major species

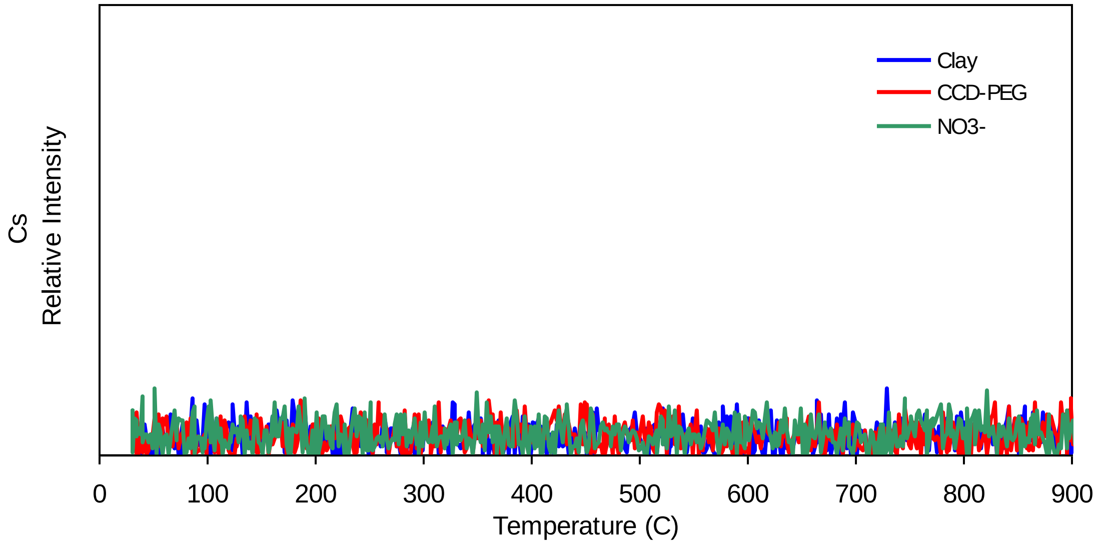

FIGURE 16 Off-gas analysis of cesium from bentonite clay (blue) and bentonite clay loaded with Cs, Sr, Rb, and Ba from the CCD-PEG (red) or nitrate (green) waste feeds.

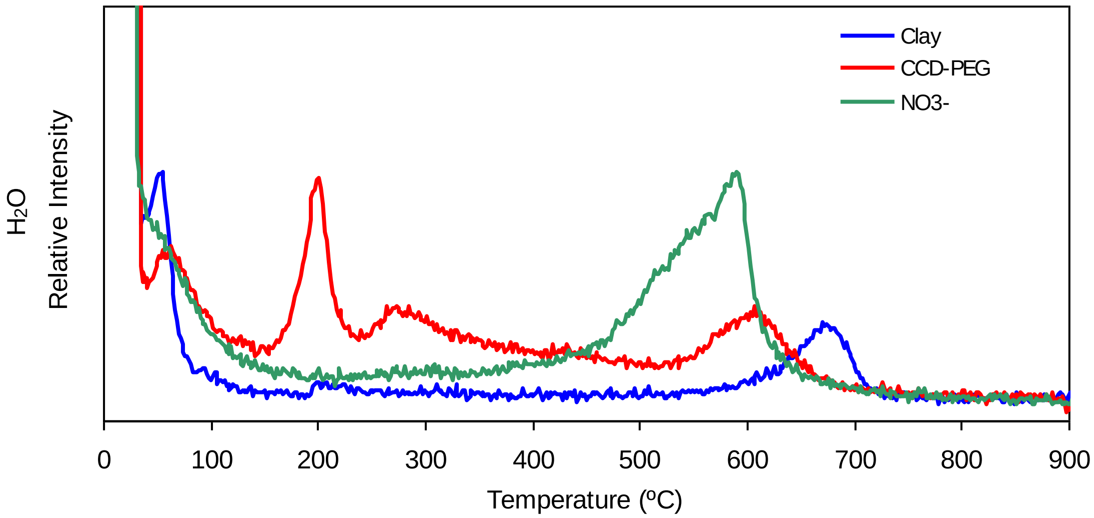

FIGURE 17 Off-gas analysis of water from bentonite clay (blue) and bentonite clay loaded with Cs, Sr, Rb, and Ba from the CCD-PEG (red) or nitrate (green) waste feeds.

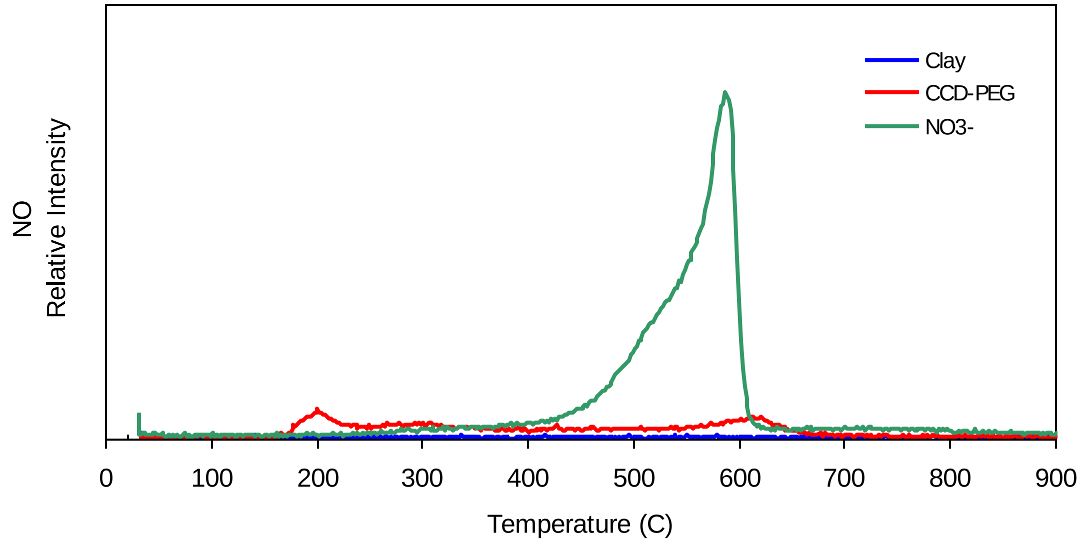

FIGURE 18 Off-gas analysis of NO species from bentonite clay (blue) and bentonite clay loaded with Cs, Sr, Rb, and Ba from the CCD-PEG (red) or nitrate (green) waste feeds.

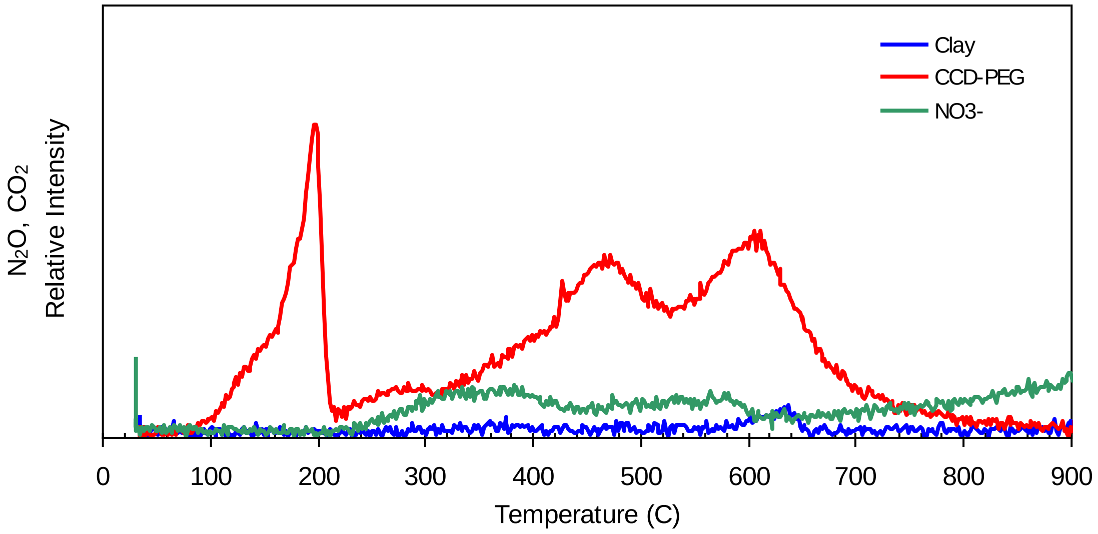

FIGURE 19 Off-gas analysis of N_2O and/or CO_2 species from bentonite clay (blue) and bentonite clay loaded with Cs, Sr, Rb, and Ba from the CCD-PEG (red) or nitrate (green) waste feeds.

3.6 THERMAL GRAVIMETRY

Weight loss and first-derivative curves from thermal gravimetric analysis of the bentonite clay loaded with the CCD-PEG waste feed are shown in Figure 20, and speciation for the mass losses was correlated with the off-gas analysis results (Table 3). Three major transitions were observed: (1) 6.2% loss at ≤100°C due to absorbed and weakly bound water, (2) 15% loss from 150-400°C corresponding to CO_2 or N_2O species and interlayer water, and (3) 14% loss of CO_2 or N_2O species and water due to dehydroxylation of the clay with a maximum peak temperature of ~600°C. The total weight loss over the range 25-800°C for the CCD-PEG waste-loaded sample corresponded to 35%.

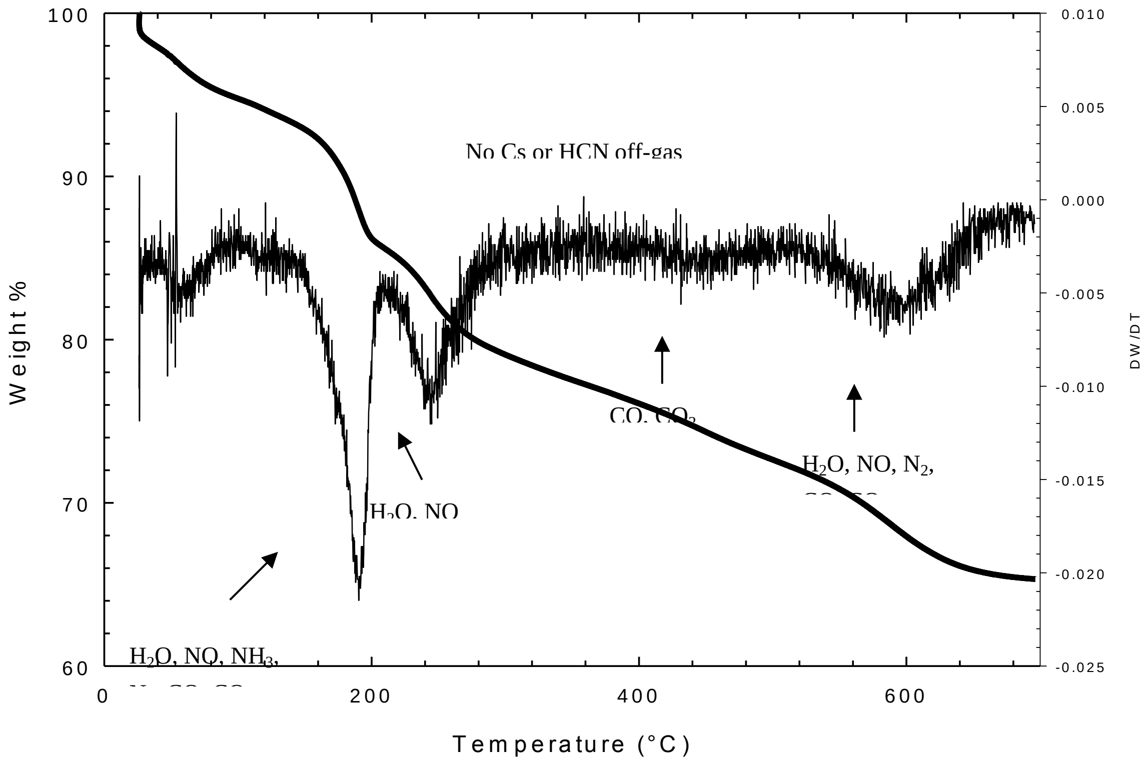

FIGURE 20 Weight loss and first-derivative curves from thermal gravimetric analysis of the CCD-PEG waste-loaded bentonite clay.

4 CONCLUSIONS

We sintered, at temperatures of 600°C to 1000°C, bentonite clay samples with up to 30 mass% of cesium, strontium, rubidium, and barium. The true density of the sintered product was 3 g/cm^3. There was an increase in porosity (~20%) with an increase in waste loading (~20%) for the chloride-waste loaded clay after sintering to 1000°C. We could not detect any loss of cesium during sintering. Instead, there was an increase in crystallinity of the waste form upon sintering to 1000°C for the chloride- and nitrate-salt loaded clays. The nitrate salt feed produced various cesium pollucite phases while the chloride salt feed did not produce these familiar phases. In fact, many of the x-ray diffraction peaks could not be matched to known phases. Assemblages of silicates were formed that incorporated the Sr, Rb, and Ba ions. Gas evolution during sintering to 1000°C was significant (35% weight loss for the CCD-PEG waste loaded clay), with significant water being evolved at approximately 600°C.

5 ACKNOWLEDGMENTS

The authors thank M. Ferrandon for the TGA analyses. This work was conducted in support of the Global Nuclear Energy Partnership Nuclear Waste Form Campaign. Argonne National Laboratory is operated for the U.S. Department of Energy by UChicago Argonne, LLC, under contract DE-AC0Z-06CH11357.

6 REFERENCES

Carrado 1991
K. Carrado, “The direct synthesis of organic-containing clays and thermal analysis of porphyrin-clay complexes,” ANL/CP-72964, presented at the ACS National Meeting, Atlanta, GA, April 14-19 (1991).

Kaminski 2005
M.D. Kaminski, “Engineered product storage under the Advanced Fuel Cycle Initiative. Part I: An iterative thermal transport modeling scheme for high-heat-generating radioactive storage forms,” J. Nucl. Mater. 347(1-2), 94-103 (2005).

Kaminski 2005
M.D. Kaminski, “Engineered product storage under the advanced fuel cycle initiative. Part II: Conceptual storage scenarios,” J. Nucl. Mater. 347(1-2), 104-110 (2005).

MacLaren 1999
I. MacLaren, J. Cirre, C.B. Ponton, “Hydrothermal Synthesis of Pollucite ($CsAlSi_2O_6$) Powders,” J. Am. Ceram. Soc. 82 (11), 3242–44 (1999).

Singh 1995
R. Singh, K.J. Singh, D.R. Chaudhary, “Heat conduction and porosity correction for diverse two-phase systems,” J. Phys. D: Appl. Phys. 28, 1573-1578 (1995).

Strachan 1976
D. Strachan, W. Shulz, “Glass and Ceramic Materials for the Immobilization of Megacurie-Amounts of Pure Cesium-137,” ARH-SA-246, April (1976).

Yanagisawa 1987
K. Yanagisawa, M. Nichioka, N. Yamasaki, “Immobilization of cesium into pollucite structure by hydrothermal hot-pressing,” J. Nucl. Sci. Technol. 24(1), 51-60 (1987).

APPENDIX

TABLE A1 Information on Cs and Sr waste form surrogates formed with chloride salts of Cs, Sr, Rb, and Ba. Dimensions for outside diameter (OD) and height (H) in inches, force in lb, volume in mL, mass in gram of element, time in h, temperature in °C, density in g/cm^3. DNM = did not measure.

Sample #	ID Die (in.)	Cold Press Force (lbs)	PSI	Sinter Time	Sinter Temp.	OD	H	Final Mass	Geometric Density	Pyc-nometer Density	Porosity	Notes
0	1-1/8	5000	5000	12	1000	DNM	DNM	DNM	DNM	DNM	DNM	Test, orange-brown
1	1-1/8	5000	5000	12	1000	1.1	0.666	16.729	1.61	3.05	47.11%	Yellow-white with black soot
2	1-1/8	5000	5000	12	1000	1.094	0.55	15.412	1.81	2.83	35.82%	Yellow-white with some black soot
3	1-1/8	5000	5000	12	1000	1.055	0.474	14.055	2.07	2.63	21.31%	Yellow-white
4	1/2	1000	5000	12	1000	0.479	0.558	2.8703	1.74	3.06	43.16%	48h between press and sinter
5	1/2	1000	5000	12	1000	0.48	DNM	4.4821	DNM	2.90	DNM	Pollucite
6	1/2	1000	5000	12	900	0.49	0.77	3.9743	1.67	3.06	45.37%	48h between press and sinter
7	1/2	1000	5000	12	900	0.486	0.7715	3.9666	1.69	3.02	43.96%	
8	1/2	3000	15000	12	1000	0.5	0.25	1.426	1.77	3.09	42.63%	2 weeks between press and sinter
9	3/4	6600	15000	12	1000	0.736	0.345	4.6832	1.95	3.05	36.14%	
10	3/4	4400	10000	12	1000	0.731	0.367	4.728	1.87	DNM	DNM	
11	3/4	2200	5000	12	1000	0.725	0.33	3.9384	1.76	DNM	DNM	
12	3/4	2200	5000	12	1000	0.73	0.345	4.4204	1.87	2.86	34.65%	Pollucite
13	1/2	1000	5000	12	800	0.511	0.815	4.1014	1.50	3.10	51.74%	
23	1/2	1000	5000	12	900	DNM	DNM	DNM	DNM	DNM	DNM	Sample discarded
24	1/2	1000	5000	12	700	DNM	DNM	DNM	DNM	DNM	DNM	Sample discarded
26	1/2	1000	5000	12	600	DNM	DNM	DNM	DNM	DNM	DNM	Sample discarded
27	3/4	2200	5000	12	800	DNM	DNM	DNM	DNM	3.08	DNM	Whitish color

TABLE A1 (Cont.)

Sample #	ID Die (in.)	Cold Press Force (lbs)	PSI	Sinter Time	Sinter Temp.	OD	H	Final Mass	Geometric Density	Pyc-nometer Density	Porosity	Notes
28	3/4	2200	5000	12	700	0.771	0.2795	3.4393	1.61	2.95	45.55%	Color less white and more skin-toned
29	3/4	2200	5000	12	600	DNM	DNM	DNM	DNM	2.94	DNM	Color less white and more skin-toned, noticeably more friable than at higher T

TABLE A2 Compositional information on Cs and Sr waste form surrogates formed with chloride salts of Cs, Sr, Rb, and Ba (% load is total elemental mass of Cs, Sr, Rb, and Ba in the clay sample).

Sample #	Waste Feed Solution Volume (mL)	Cs (g)	Sr (g)	Rb (g)	Ba (g)	Clay mass (g)	% load
0	0						
1	27.9	2.10	1.05	0.33	2.75	14.996	29.4
2	13.95	1.05	0.52	0.17	1.37	15.996	16.3
3	6.975	0.52	0.26	0.084	0.69	16.996	8.4
4	27.9	2.10	1.05	0.33	2.75	14.9932	29.4
5	13	9.79	0	0	0	15.0027	39.5
6	27.9	2.10	1.05	0.33	2.75	14.9932	29.4
7	27.9	2.10	1.05	0.33	2.75	15.0058	29.3
8	27.9	2.10	1.05	0.33	2.75	14.9932	29.4
9	27.9	2.10	1.05	0.33	2.75	15.0058	29.3
10	27.9	2.10	1.05	0.33	2.75	15.0058	29.3
11	27.9	2.10	1.05	0.33	2.75	15.0058	29.3
12	13	9.79	0	0	0	15.0027	39.5
13	27.9	2.10	1.05	0.33	2.75	15.0058	29.3
23	27.9	2.10	1.05	0.33	2.75	14.9932	29.4
24	27.9	2.10	1.05	0.33	2.75	14.9932	29.4
26	27.9	2.10	1.05	0.33	2.75	14.9932	29.4
27	27.9	2.10	1.05	0.33	2.75	14.9941	29.4
28	27.9	2.10	1.05	0.33	2.75	14.9941	29.4
29	27.9	2.10	1.05	0.33	2.75	14.9941	29.4

Nuclear Engineering Division
Argonne National Laboratory
9700 South Cass Avenue, Bldg. 208
Argonne, IL 60439-4854

www.anl.gov